

PS6-5 – 6156

Modeling the structural fumigation of flour mills and food processing facilities

W. Chayaprasert¹, D.E. Maier¹, K.E. Ileleji¹, J.Y. Murthy²

Abstract

3D computer models for structural fumigation were developed based upon comprehensive data sets collected at a fumigation job in a commercial flour mill. The fumigation models were divided into two parts: internal and external flow models. The external flow model, which included the flour mill and surrounding structures, was used to predict stagnation pressures on the mill's walls as a function of the wind speed and direction data. The pressure differences due to density differences between the gas inside and the air outside of the mill (stack effect) were also estimated using the environmental temperature and relative humidity data. The combined effect of the stagnation pressure and the stack effect was used for estimating the boundary conditions of the internal flow model. The internal flow model incorporated interior details of the mill such as building plans, locations of major equipment, partitions, piping and ducting. The idea of representing the cracks as an effective leakage zone was adopted. The internal flow model was able to yield a half-loss time (HLT) close to the HLT derived from the field trial data. Therefore, it was concluded that the models were valid and the modeling

methodology established could be utilized for structural fumigation modeling in any type of structure.

Key words: Structural Fumigation Modeling, Methyl Bromide Alternative, Sulfuryl Fluoride, Half-Loss Time, Computational Fluid Dynamics.

Introduction

The phase-out of methyl bromide (MB) as the major fumigant for use in structural fumigation has warranted the industry to seek for alternative pest control measures. However, fumigation with other MB alternatives is more costly and requires a higher level of stewardship to be economically competitive. Therefore, the key for successful adoption of these alternatives lies in the efficiency of its application during fumigation. Because it is not practical to perfectly seal the structure, the fumigation process can be better optimized only if the dynamics of gas movement in the fumigated space and the effects of environmental conditions on the process are well understood.

The decay of fumigant concentration is mainly due to the transfer between the fresh air outside

¹ Graduate Research Associate, Department of Agricultural and Biological Engineering, Purdue University, 225 South University Street, West Lafayette, Indiana, 47907 USA.

² Professor and Extension Engineer, Department of Agricultural and Biological Engineering, Purdue University, 225 South University Street, West Lafayette, Indiana, 47907 USA. Fax: (765) 496-1356, E-mail: maier@purdue.edu

³ Assistant Professor and Extension Engineer, Department of Agricultural and Biological Engineering, Purdue University, 225 South University Street, West Lafayette, Indiana, 47907 USA

⁴ Professor, Department of Mechanical Engineering, Purdue University, 585 Purdue Mall, West Lafayette, Indiana, 47907 USA

and the fumigant-air mixture in the fumigated space. These movements are created by pressure differences across the building envelope. Hence, the analysis of fumigant gas leakage is similar to that of infiltration through an air-tight building. Two main forces that create pressure differences across the building envelope driving natural ventilation and infiltration are the wind and stack (or buoyancy) effects (Ashrae, 2001). The combination of these two effects characterizes each building and complicates the analysis. Thus, the Computational Fluid Dynamics (CFD) method is a proper method to solve this type of problem. In the heating, ventilation, and air conditioning (HVAC) industry, it has been used to study wind-induced pressure on building surfaces (Burnett et al., 2005; Senthoran et al., 2004) and contamination in building spaces (Cheong et al., 2003; Gilham et al., 2000; Sekhar and Willem, 2004). Additional studies by other researchers have also been published on these topics. However, no published study has been found in the literature on the use of the CFD method for modeling the fumigation process in large structures.

This study was the first phase of an effort to develop an analysis tool for structural fumigation and a precision fumigation controller that can automatically apply and regulate fumigant gas during fumigation. The primary objective of this study was to develop flow models for prediction of fumigant leakage and distribution during the fumigation process in a reference flour mill. The specific objectives were to use a commercial CFD solver, Fluent[®] (Fluent Inc., Lebanon, NH): 1) to construct a model of the flow outside the reference structure for predicting stagnation pressure profiles on the structure's walls created by prevailing wind, and 2) to construct a model of the fumigation process that is able to reproduce concentration data similar to those observed during an actual fumigation job conducted in the reference structure.

The model development process was based on the hypothesis that an acceptable model should be able to reproduce concentration data that predicts HLT values similar to those

observed from experimental concentration data, given the same environmental conditions and fumigation practices. A fumigation experiment was conducted as part of a commercial structural fumigation in a grain processing facility in order to collect experimental data necessary for validating the CFD models. The experiment and the resulting data are described in the paper entitled Real-time Monitoring of a Flour Mill Fumigation with Sulfuryl Fluoride by the same authors.

Material and methods

External flow model

The domain of the external flow model was set-up as a rectangular volume such that it included the grain processing building and the surrounding structures. The perimeter boundaries for the upwind side were specified as velocity inlets and the boundaries for the downwind side were specified as pressure outlets. To represent the atmospheric boundary layer, the velocity profile at the inlet boundary(ies) is calculated as (Ashrae, 2001)

$$U_H = U_{met} \left(\frac{\delta_{met}}{H_{met}} \right)^{\alpha_{met}} \left(\frac{H}{\delta} \right)^{\alpha} \quad (1)$$

where U_H is the local wind speed (m/s) at height H (m) and U_{met} is the meteorological wind speed (m/s) measured at height H_{met} (m). The descriptions and values for the other parameters can be found in Ashrae (2001). Uniform static pressure with a value of 0 Pascal was specified at the pressure outlet boundary(ies).

Results

Several steady-state flow simulations were conducted with different fixed wind speeds and directions. The wind directions were specified

between 0 and 360 degrees with 15 degree intervals. At each direction, six simulations were conducted with six wind speeds: $U_{met} = 1, 2, 4, 6, 8,$ and 10 m/s.

Figure 1.a displays the resulting stagnation pressure profile when U_{met} was 4 m/s coming from a 30 degree angle with respect to the North. The experimental wind data however were measured at the grain processing building's roof and for this particular case the wind speed at the building's roof was 4.1 m/s. The average stagnation pressures on the north, east and west walls were calculated separately using the pressure values and the wall areas shown in the figure. These average pressures were then plotted against the wind speed calculated at the building's roof (Figure 1.b). The average pressures from the simulations with the other boundary wind speeds ($U_{met} = 1, 2, 6, 8,$ and 10 m/s) were also plotted. It was found that the relationship between the roof wind speeds and the stagnation pressures for each wall was a second order polynomial fit ($R^2 \approx 1$). Similar results were found for the other wind directions. The coefficients of the fits were unique for every wind direction. Thus, at a fixed wind direction average stagnation pressures on the north, east

and west walls could be calculated for any roof wind speed.

Average stagnation pressures on the north, east and west walls of the flour mill as a function of wind speed. The values labeled 1, 2 and 3 are average pressure values corresponding to the magnified frames with the same numbers in (a).

The average stagnation pressures on the east wall as a result of all external flow simulations were comprehensively illustrated in Figure 2. These values were calculated using the polynomial fits that were derived from the external flow simulation results. Similar charts were also created for the north and west walls (data not shown). In general, regardless of wind directions, the stagnation pressures on all walls, when the wind speed was 1 and 2 m/s, were substantially lower (approximately within ± 1 Pascal) as compared to those for the higher wind speeds.

By mapping the plot in Figure 3 with the experimental wind speeds and directions, the average stagnation pressures that would have occurred on the east wall during the fumigation period could be estimated. The average stagnation pressures on the north and west walls could be estimated using the same procedure.

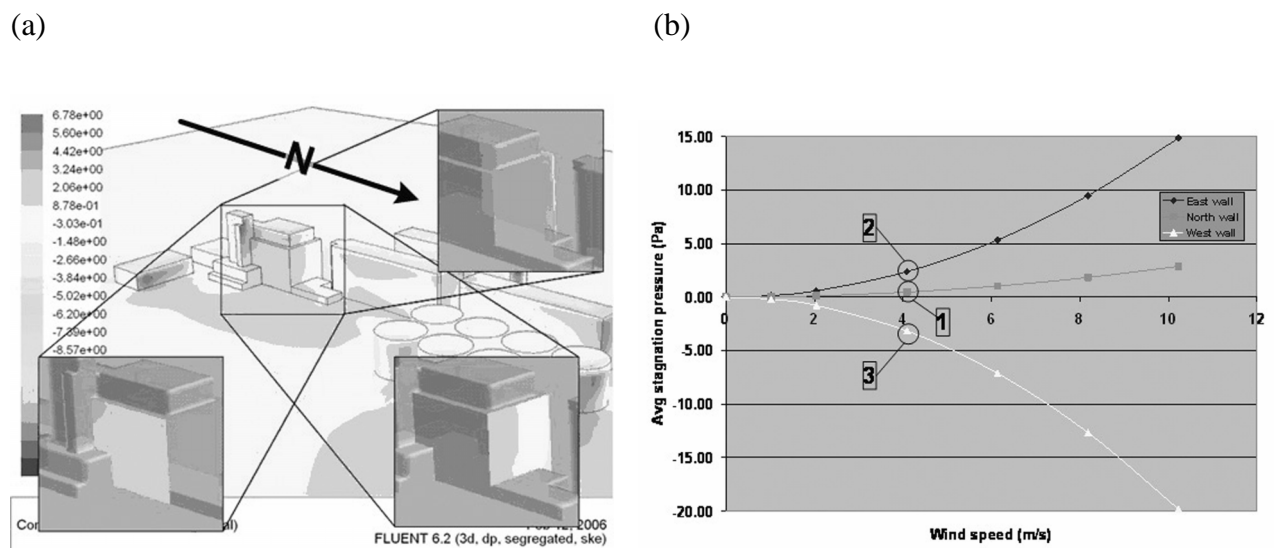


Figure 1. Results of the external flow simulations when the wind direction was fixed at 30 degrees with respect to the North. (a) Stagnation pressure contour on the building's surfaces when $U_{met} = 4$ m/s. The magnified frames labeled 1, 2 and 3 indicate the regions that were used to calculate average pressures on the north, east and west walls, respectively. (b)

Figure 3 displays time series of the resulting average pressures on the north, east and west walls during the fumigation period. Most of the time, positive pressures were exerted on the east wall and the opposite occurred on the north and west walls. The average pressures on the north wall were almost zero between the sixth and eleventh hours. Beginning at the eighteenth hour, the means of the average pressures on all walls were predicted to decrease. These pressure series

were used as boundary conditions of the internal flow model which will be described in the next section.

Note that the pressures on the south wall of the flour mill were not taken into consideration because the south side of the flour mill is not exposed to the external environment. Instead, it is attached to the packaging building. During the fumigation, the walkway between the two structures was sealed and thus it was assumed that no gas movement occurred through the south wall of the mill.

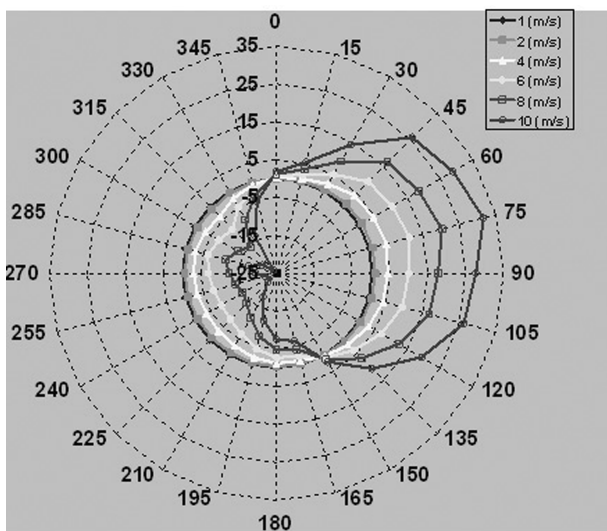


Figure 2. Average stagnation pressures on the east wall as calculated using the polynomial fits that were derived from the external flow simulation results.

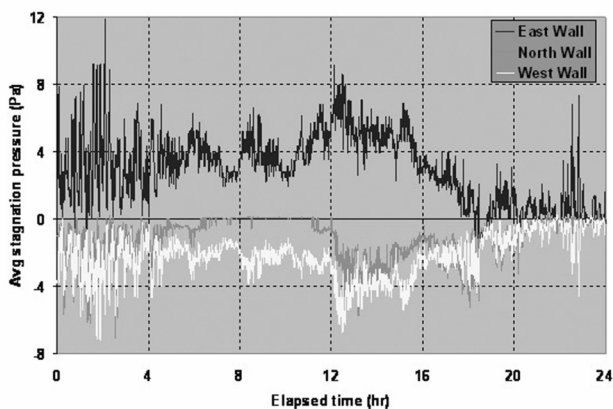


Figure 3. Predicted average stagnation pressures on the north, east and west walls during the fumigation period. Elapsed time zero, 0, indicates the time of the first fumigant release.

Internal flow model

Unlike the external flow model, the dynamics of fumigant concentrations indicates that the flow of a gas fumigant inside a structure is an unsteady state problem. In the fumigation experiment, gas movement between the fifth and sixth floors of the mill and between the mill and the other connecting structures were minimized by sealing the air pathways between them. Assuming that these air pathways were perfectly sealed, the domain of the internal flow model included only the first five floors of the mill. The domain contained rectangular solid volumes representing milling equipment such as rollermills, purifiers, sifters, pneumatic cyclones, tanks and tempering bins. The locations of the fumigant introduction sites and circulation fans in the model were approximately the same as the actual locations documented from the experiment. The rate at which the fumigant (ProFume[®]) was released was calculated using an estimated formula (Prabhakaran, 2005). A constant flow rate of 2.71 m³/s was assumed for all circulation fans in the model. Figure 4 shows the domain of the internal flow model. The total dimensions of the domain were 26.5 m x 34.4 m x 27.6 m.

According to Ashrae (2001), the stack pressure difference for a horizontal leak at any vertical location can be calculated as:

$$\Delta p_s = (\rho_o - \rho_i)g(H_{NPL} - H) \tag{2}$$

where r_o and r_i are the outdoor and indoor air

densities (kg/m^3), respectively, g is the gravitational constant (9.81 m/s^2), and H is the height above a reference plane (m). H_{NPL} is the height of the neutral pressure level (NPL) above the reference plane (m). In this study, H_{NPL} was assumed to be the middle height of the flow domain (13.8 m). Using Equation 2, the equivalent pressure differences due to the stack effect were calculated along the height of the flour mill. The outdoor density was determined by applying the psychrometric relationship to the experimental data of barometric pressure, temperature, and RH. The indoor air density was substituted with the density of the fumigant-air mixture which was the mass integration of the fluid within the flow domain.

To model leakage, it was assumed that the leakage of fluid through all cracks on a wall can be equivalently represented by the leakage through an equivalent leakage zone (ELZ). An ELZ was a pressure boundary condition with an assumed area (effective leakage area) and a loss coefficient. The pressure drop across the effective leakage area was calculated by:

$$\Delta p = k_L \frac{1}{2} \rho v^2 \quad (3)$$

where r is the fluid density (kg/m^3), n is the

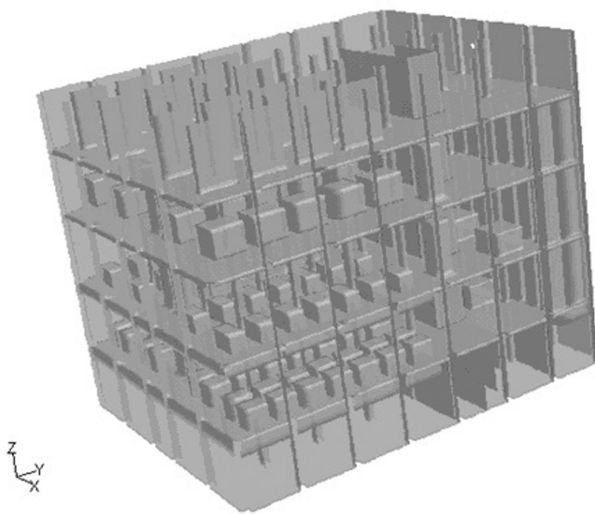


Figure 4. The internal flow domain of the first five floors of the flour mill.

velocity through the vent (m/s), and k_L is the loss coefficient. The effective leakage area for the ELZ was arbitrarily chosen as a circle with a diameter of 0.43 m. Five ELZs were placed on each of the north, east and west walls. Each ELZ was positioned at the middle of the wall on each floor. As mentioned earlier, it was assumed that there was no leakage through the south side of the mill and therefore no ELZ was placed on the south wall. It was also assumed that the loss coefficients, k_L , of all ELZs were identical. At each simulation time step, the pressure value assigned to each ELZ was a summation of the average stagnation pressure, which was different for different walls, and the stack effect pressure, which varied with the height of the ELZ. A time step of 3 minutes was selected for the internal flow simulations because it yielded a reasonable computer run time.

Discussion

Equation 3 implies that k_L is an indication of the gas-tightness of the mill envelope. It is a property of the mill and does not change with weather conditions. However, it is affected by the quality of the sealing method. With the pressure inputs having been determined from the external flow simulations, the amount of leakage can be controlled by adjusting the k_L value of the ELZs. Several internal flow simulations were performed with different k_L values. At each simulation time step, fumigant concentrations in the flow domain were recorded at the same monitoring locations as in the actual mill.

The simulation result that was closest to the experimental concentration data is shown in Figure 5 which illustrates the simulated concentration curves of all monitoring points (18) in the first five floors when k_L was equal to 90. The lower-case “m” in the labels indicates that these curves were simulated data. The primary discrepancies observed between the field trial data and the simulation data were in the fumigant introduction phase. In the simulation, there were fewer differences in the peak concentrations

among the floors. Comparing floor by floor, the experimental peak concentrations on the first and second floors were higher than the simulated peak values. The opposite occurred on the fourth and fifth floors. The simulated peak concentrations on the third floor were between the peak concentrations measured by the two Fumiscopes. This resulted in much less time for uniform gas distribution. The differences in the simulated concentrations at all locations were within 5 g/m^3 at the fourth hour, while the same occurred approximately at the sixth hour in the field trial. In addition, unlike the field trial data, the simulated concentrations at m5_1, m5_3, and m5_4 reached the equilibrium as quickly as those at the other monitoring locations. These discrepancies were

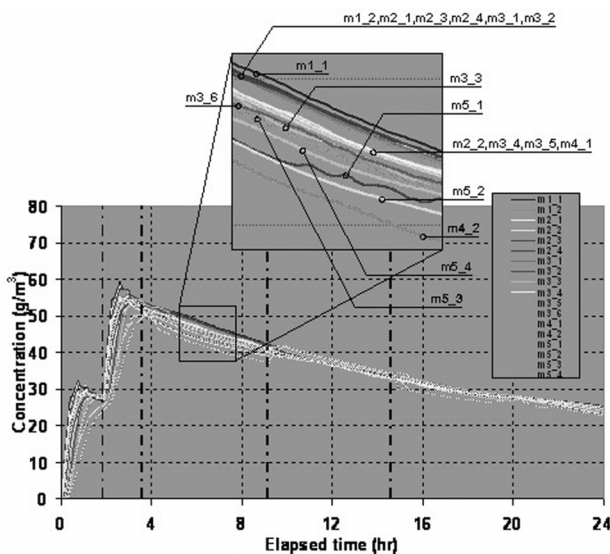


Figure 5. ProFume[®] concentrations obtained from the internal flow model with $k_L = 90$. The 0th and 24th hours are the times when the first ProFume[®] introduction started and the mill was unsealed, respectively. The first dash-dotted line (1.80) is when the second ProFume[®] introduction started. The second and fourth dash-dotted lines (3.51 and 14.50) are when the fans on the second, third and fourth floors were turned off. The third dash-dotted line (9.05) indicates when these fans were turned on.

anticipated mainly due to the simplification of the flow domain. Neglecting the fifth floor data, during the first fan-off period the fumigant in the simulation was not as well mixed as in the field trial. For this particular case, the greatest difference between the highest (m1_1) and lowest (m4_2) concentrations was approximately 6 g/m^3 or a difference of about 12 to 15%. This underprediction of mixing was anticipated due to the lack of modeling the convective currents in the model. However, the underprediction was not considered critical because on average the model was able to yield a HLT value close to the HLT derived from the experimental data as discussed in the next paragraph. Once the second, third and fourth floor fans were restarted, the flow field was dominated by momentum again and the fumigant quickly equilibrated. During the second fan-off period, the concentration differences within the mill were still insignificant (within 3 g/m^3 difference). The simulations with the other k_L values (data not shown) showed similar observations, except that the peak concentrations slightly decreased as the k_L value decreased.

The average of all concentration curves in Figure 5 is plotted as the smooth solid curve in Figure 6a. When the data between the third and eighteenth hours of the average simulated concentration curve were fitted with the theoretical concentration decay equation (Equation 1 in the Real-time Monitoring of a Flour Mill Fumigation with Sulfuryl Fluoride paper by the same authors), the simulated mill presented a HLT of 17.33 hours ($R^2 > 0.995$), which was essentially identical to the calculated 17-hour HLT of the actual mill. The curve with markers shown in Figure 6a indicates average concentrations calculated using the experimental readings. Comparing the two average curves in Figure 6a, most of the time the model slightly underpredicted the concentration levels. This resulted in the underprediction of the Ct product as illustrated in Figure 6b. At the time of unsealing, the Ct products (i.e., area under the curve) of the experimental and simulated data were approximately 950 and 850 g-hr/m^3 , respectively, or a difference of 10.5 %.

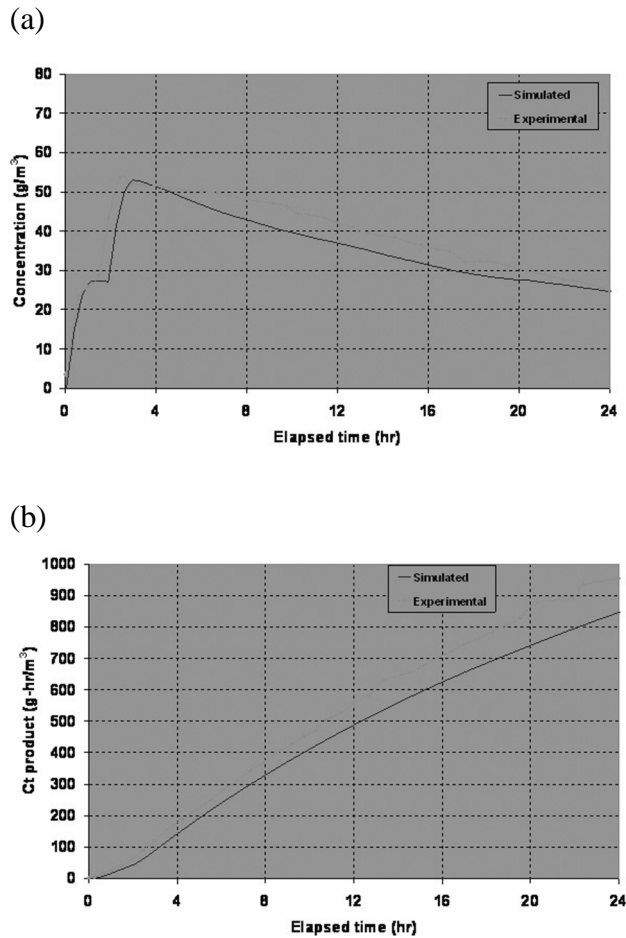


Figure 6. Comparison between the mill trial and simulation results. (a) Average concentration plot. (b) Average Ct product plot.

Conclusions

This research presented a methodology for using a commercial CFD solver, Fluent®, to model the fumigation process in a flour mill based on a data set collected at an actual fumigation site. The simulation illustrated several minor discrepancies from the experimental results. However, the final achieved Ct product was underpredicted by only 10.5%. Furthermore, the HLT values derived from the internal flow model result and the field trial data were essentially the same (17 hours). Therefore, the CFD models developed in this study were valid and the established methodology could be utilized for fumigation process modeling in any type of structure.

Given weather conditions, the models can be used to predict fumigation characteristics such as fumigant movement paths, concentration distributions, and leakage rate. The effects of fumigation variables such as wind speed and direction, capacity and placement of circulation fans, and fumigant release time on the efficacy of the fumigation process are currently being evaluated. The results from the simulations will provide insight into understanding the dynamics of the structural fumigation process and help fumigators to correctly determine the amount of fumigant to be used, which in turn will yield increased efficacy and more successful fumigation jobs.

Acknowledgments

This study was funded by the USDA-CSREES Methyl Bromide Transition Program under project grant 2004-51102-02199 “Fumigation Modeling, Monitoring and Control for Precision Fumigation of Flour Mill and Food Processing Structures.” The cooperation, input and help of Mr. John Mueller, Mr. David Mueller, Mr. Peter Mueller and the staff of Fumigation Service & Supply Inc., Indianapolis, Indiana has been greatly appreciated throughout this project. The cooperation of Dr. Suresh Prabhakaran, Mr. Marty Morgan and other staff at Dow AgroSciences, Indianapolis, Indiana, as well as the staff of several flour mills is also acknowledged.

References

- Ashrae, 2001. ASHRAE Handbook - Fundamentals. Atlanta, GA: American Society of Heating, Refrigerating and Air-Conditioning Engineers, Inc.
- Burnett, J., Bojic, M., Yik, F., 2005. Wind-induced pressure at external surfaces of a high-rise residential building in Hong Kong. *Building and Environment* 40, 765-777.

- Cheong, K.W.D., Djunaedy, E., Poh, T.K., Tham, K.W., Sekhar, S.C., Wong, N.H., Ullah, M.B., 2003. Measurements and computations of contaminant's distribution in an office environment. *Building and Environment* 38, 135-145.
- Gilham, S., Deaves, D.M., Woodburn, P., 2000. Mitigation of dense gas releases within buildings: validation of CFD modelling. *Journal of Hazardous Materials* 71, 193-218.
- Sekhar, S.C., Willem, H.C., 2004. Impact of airflow profile on indoor air quality - a tropical study. *Building and Environment* 39, 255-266.
- Senthooran, S., Lee, D.-D., Parameswaran, S., 2004. A computational model to calculate the flow-induced pressure fluctuations on buildings. *Journal of Wind Engineering and Industrial Aerodynamics* 92, 1137-1145.
- Prabhakaran, S., 2005. Personal communication with Dr. Suresh Prabhakaran, Bio/Technical Expert, Dow AgroSciences, Indianapolis, Indiana. 20 June 2005.